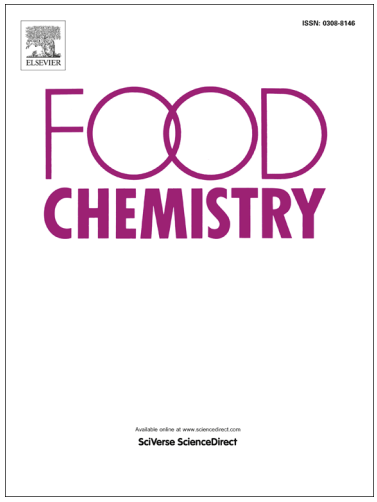

An efficient fluorescence resonance energy transfer system from quantum dots to graphene oxide nano sheets: application in a photoluminescence aptasensing probe for the sensitive detection of diazinon

Majid Arvand, Aazam A. Mirroshandel

PII: S0308-8146(18)32173-3
DOI: https://doi.org/10.1016/j.foodchem.2018.12.069
Reference: FOCH 24028

To appear in: *Food Chemistry*

Received Date: 9 July 2018
Revised Date: 27 November 2018
Accepted Date: 13 December 2018

Please cite this article as: Arvand, M., Mirroshandel, A.A., An efficient fluorescence resonance energy transfer system from quantum dots to graphene oxide nano sheets: application in a photoluminescence aptasensing probe for the sensitive detection of diazinon, *Food Chemistry* (2018), doi: https://doi.org/10.1016/j.foodchem.2018.12.069

An efficient fluorescence resonance energy transfer system from quantum dots to graphene oxide nano sheets: application in a photoluminescence aptasensing probe for the sensitive detection of diazinon

Majid Arvand*, Aazam A. Mirroshandel

Analytical Chemistry Laboratory, Faculty of Chemistry, University of Guilan, Namjoo Street, P.O. Box 1914, Rasht, Iran

*Corresponding author. Tel.: +98 13 33320912, fax: +98 13 33333262

E–mail address: arvand@guilan.ac.ir

Abstract

In this paper a new aptasensor with high-sensitivity, and high-specificity for detection of diazinon, was discovered, based on fluorescence resonance energy transfer (FRET) between quantum dot (QD) as a donor and graphene oxide (GO) as an acceptor. L-cysteine capped CdS QDs/DF20 aptamer bioconjugates were successfully synthesized. GO was also attached to aptamers and photoluminescence quenching was obtained through FRET. By adding target diazinon to the bioconjugates containing GO, photoluminescence recovery was detected due to detachment of GO from the aptamer as a result of the difference in affinity for the aptamer. The detection limit of the biosensor was 0.13 nM and the linearity was maintained from 1.05 to 206 nM. Other pesticides and herbicides did not contribute to photoluminescence recovery due to lack of binding affinity for the aptamers, which demonstrates the selectivity of the biosensor. The results show the applicability of the aptasensor for monitoring diazinon in environmental and agricultural samples.

Keywords: Aptamer; Graphene oxide; Diazinon; Quantum dot; Fluorescence resonance energy transfer

1. Introduction

Organophosphorus compounds (OPs) are primarily used in agriculture as pesticides. OPPs have replaced organochlorine compounds due to the durability and accumulation of the latter in the environment (Bavcon et al., 2003). Diazinon [O, O-diethyl-O-(2-isopropyl-4-methyl-6-pyrimidyl) phosphorothioate] is an organophosphorus pesticide that is widely used in agricultural and non-agricultural applications (Sullivan & Goh, 2000). After diazinon is applied, it is often found in the surrounding soil and surface waters, as well as on the surface of plants. Therefore, it is important to check the concentrations of pesticides and their metabolites in environmental samples. Usually OP compounds are detected in different samples by chromatographic methods, such as high performance liquid chromatography (HPLC) and liquid chromatography/gas chromatography-mass spectrometry (LC/GC-MS), or spectrophotometric assays that are based on cholinesterase inhibition (Ma et al., 2009). The accuracy of these technologies varies, and HPLC is best. However, these methods are laborious and time-consuming as well as requiring sample pretreatment and highly trained professional personnel.

Various simple and novel biosensors have been constructed for the assessment of OP compounds, using aptamer as a biorecognition element in combination with various transduction schemes, such as electrochemical approaches (Sotiropoulou et al., 2005), optical methods (Vamvakaki & Chaniotakis, 2007), and micro cantilever (Karnati et al., 2007) or colorimetric assays (Hossain et al., 2009).

Semiconductor nanocrystals, or quantum dots (QDs), are among the most exciting and agreeable discoveries that have emerged from the nanotechnology field. A QD is a cluster of a few hundred to thousands of atoms arranged in binary (*e.g.* CdSe, CdTe, GaAs, InAs, AlN, and SiC) or ternary compounds (*e.g.* InGaN, InGaP, and InGaAs) (Zhang & Wang, 2012; Freeman &

Willner, 2012). The QDs have been used as excellent fluorescent labels in FRET-based sensors (Huang et al., 2014; Geibler & Hildebrandt, 2016). By combination of QDs to different biomolecules, such as aptamers, FRET could be used for the fabrication of aptasensors (Shi et al., 2015).

Aptamers are single-stranded oligonucleotides with specific sequences (DNA or RNA molecules). They are capable of recognizing and binding to their cognate targets with high affinity and specificity (Liu et al., 2016; Li et al., 2015). Among many new aptamer-based sensors, and aptasensors, GO-based aptasensors have attracted great interest, mainly for biosensing utilization. A significant property of GO, which allows us to discover aptasensors, is its major affinity for single-stranded DNA (ssDNA). In contrast, GO shows little affinity for a complex formed by recognizing a target molecule (Tang et al., 2017).

The QDs at the aptamer terminus leave the GO surface when the target is present. Another favourable feature of GO for biosensors is that the sp^2 domain of the GO behaves as an effective quencher for FRET (Treossi et al., 2009).

FRET is the state-of-the-art technique that can be used for high-sensitivity and high-specificity detection of a target protein, DNA, and other specific molecules. FRET demonstrates energy transfer from a donor to an acceptor. As a result, it occurs only when their respective energy emission and absorption bands overlap with each other (Gang-Il et al., 2009). The absorption spectrum of GO covers a broad range of wavelengths (approximately 300-700 nm), overlapping the fluorescence spectra of QDs, in good accordance with literature results (Dong et al., 2010).

Here, we report a photoluminescence aptasensor for the selective detection of diazinon, based on FRET. In the absence of target, the QDs-labelled aptamer was adsorbed onto the GO surface

and the fluorescent signal was quenched. Upon addition of diazinon, it bound to the aptamer which would remove the QDs/aptamer ensembles far away from the GO surface and cause a fluorescent signal recovery. As a result, the fluorescent signal of the aptasensor depended on the concentration of diazinon. The optimized condition and the selectivity of the aptasensor towards diazinon were also studied. Furthermore, the aptasensor was used to detect diazinon in environmental and agricultural samples.

2. Materials and methods

2.1. Materials

An ssDNA aptamer for diazinon, reported previously, was employed as the targeting ligand (Jokar et al., 2017). The sequence of the modified aptamer (DF20) was 5′-NH_2-C6-ATCCGTCACACCTGCTCTAATATAGAGGTATTGCTCTTGGACAAGGTACAGGGATGGTGTTGGCTCCCGTAT-3′. DF20 with the complete sequence was synthesized from Bioneer® Corporation, Republic of Korea by Optical Density 4 OD, T_m= 79.4 °C, Purification: PAGE. All reagents were of analytical grade and obtained from commercially available suppliers (Merck KGaA and Sigma Aldrich) and used without further purification.

2.2. Apparatus

Fluorescence spectrophotometer FP-6200 (Jusco, Japan) was used to obtain the fluorescence emission spectra, with an excited slit and emission slit of 5 nm and excitation wavelength of 278 nm. Transmission electron microscope (TEM) images were acquired on an EM10C (Zeiss-Germany) transmission electron microscope operating at 80 kV. Characterization of the morphology of the QDs was carried out by a field emission scanning electron microscope (FE-

SEM; TESCAN MIRA). Fourier transform infra-red (FT-IR) spectra were recorded by FT-IR-8400 Shimadzu Fourier transform spectroscopy. A Philips PW1840 diffractometer with CuK_α radiation was used to record the powder XRD patterns of the QDs sample.

2.3. Preparation of GO

Pure graphite powder was used for GO synthesis by a modified Brodie method (Brodie, 1860). Briefly, 1.0 g of pure graphite powder and 8.0 g of potassium chlorate were mixed with 20 ml fuming nitric acid at room temperature without subsequent aging and stirred for 24 h. The other processes, such as washing, filtration, and cleaning were performed as in the Brodie method. The synthesized graphite oxide (10 mg) was dispersed in 30 ml of aqueous NaOH solution at alkaline pH 10. The collected graphite oxide was sonicated by a bath-type sonicator (Sonoswiss SW3-H, 38 kHz, Switzerland) for 1 h. After ultra-sonication, samples were immediately precipitated by a centrifuge at 15,000 rpm for 10 min. The GO sheets were extracted carefully.

2.4. Preparation of aptamer-conjugated QDs

The procedure described by Chen & Rosenzweig (2002), for the preparation of l-cysteine-capped CdS nanoparticles was modified and used to prepare nanoparticles; 0.5 mmol Cd $(NO_3)_2$ and 1 mmol L-cysteine were dissolved in 100 ml of deionized water and purged with pure argon gas for at least 60 min under magnetic stirring. Then, 10 ml of 0.02 M $Na_2S{\cdot}9H_2O$ solution were slowly added into the vortex of the solution, using a syringe pump at a flow rate of 0.5 ml min^{-1}. The QDs solution was refluxed while boiling for 10 h. The solution was then condensed by solvent evaporation to 20 ml. Ethanol was used to precipitate the QDs. To remove contaminants,

the precipitate of nanoparticles was treated with three repeated cycles of precipitation by adding cool ethanol, washing, and redispersion.

Aptamer surface-modified QDs were prepared by the following procedure: The carboxylic groups on the surface of the QDs were coupled to the amine-modified aptamer according to ethyl (dimethyl amino propyl) carbodiimide/N-hydroxysuccinimide (EDC/NHS) chemistry (Sheng et al., 2012). Further, the QDs (8 μM) were activated using EDC (400 mM) and NHS (40 mM) in 400 μl of 100 mM phosphate buffered saline (PBS, pH 7.0) by sonication for 10 min. This process was done in order to prepare a homogeneous solution and prevent the aggregation of the QDs. The mixture was incubated in the dark at room temperature for 1 h. The reaction mixture was then centrifuged at 13,000 rpm for 30 min. The supernatant was gradually removed and checked to confirm that there was no fluorescence. The pellet was then washed twice and dispersed in PBS buffer solution (pH 7). Then, the resulting activated QDs solution was mixed with 120 μl of 80 μM amine modified aptamer. The QDs: aptamer ratio in this process was 1:20. To form a homogeneous solution, mixture solution was sonicated for 5 min and followed by gentle shaking (i.e., 200 rpm) at 4 °C, for 18 h in a dark place to allow the coupling of the amine-terminated aptamer to the activated carboxylic groups on the surface of the QDs. The unreacted aptamers were removed by centrifugation at 13,000 rpm for 30 min. The supernatant was checked again to ensure that there was no fluorescence. The pellet was washed three times with 400 μl of 50% ethanol and dried in air for 10 min. In the final stage, the pellet was stored at 4 °C in a dark place prior to use.

2.5. Preparation of GO/aptamer-QDs ensemble and detection of diazinon

To couple the QDs with GO through ssDNA, 270 mg l^{-1} of GO were added to the aptamer-QD conjugates (100 nM) in PBS, and the fluorescence intensity was monitored after 30 min. The fluorescence intensity of QDs-aptamer can be efficiently quenched by GO due to FRET between QDs and GO.

A sensing system, consisting of aptamer/CdS QDs, GO, Na^+ (150 mM) and PBS buffer (pH 7, 100 mM) was operated as the aptasensor. Different concentrations of diazinon were added to the sensing system, respectively. The final assay solutions with a volume of 3 ml were used for the photoluminescence measurement under the 278 nm excitation. In the presence of diazinon, the fluorescence intensity was recovered and a significant fluorescence enhancement was observed. This phenomenon indicated that the competitive binding of the diazinon with GO for QDs-aptamer resulted in desorption of the QDs-aptamer from the surface of GO. The change in the fluorescence intensity of the sensing system was appraised for quantification of diazinon.

2.6. Preparation of the spiked real samples

To demonstrate the ability of this aptasensor to detect diazinon in real samples, we selected environmental and agricultural samples, including surface water, cucumber and apple as the sample matrix. A detailed procedure for the sample preparation was performed as follows:

Surface water sample was taken from Shafa-rood (Guilan, Iran) river. The water samples (10 ml) were filtered through filter paper (11 μm), and were spiked with 10, 50, and 100 nM diazinon. For the analysis of fruit samples, cucumber and apple were purchased from a local shop. The samples were washed with tap water and homogenized in a blender. 2.0 g of the homogenized sample were weighed and spiked with 10, 50, and 100 nM diazinon. 4 ml of water were added to the samples and placed in a water bath at 45 °C for 20 min, and finally centrifuged

for 10 min at 5000 rpm. The clear supernatant was collected, in order to reduce the matrix effect; it was diluted (1:2) with water (Saraji et al., 2013).

3. Results and discussion

3.1. Characterization of the prepared GO

FT-IR was employed for characterizing the surface groups and structure of graphite oxide and GO (Fig. 1A). These spectra indicate the existence of abundant oxygen-containing functional groups on GO. As shown in Fig. 1B, the sheet-like micro-structures, occasional folds, wrinkles, ultrathin features, and rolled edges of GO can be shown clearly with a TEM image of the as-synthesized GO sheet. A typical SEM image of the acceptor (i.e., GO) is shown in Fig. 1C. It is clearly revealed that the GO is uniform in size. All these results suggested the successful synthesis of GO.

3.2. Microstructure of l-cysteine-capped CdS QDs

TEM was employed to confirm direct information about the size, shape, and the morphology of L-cysteine-capped CdS nanoparticles. Fig. 1D shows that the QDs possess high monodispersity and nearly spherical shape; mean size was about 5 nm. Fig. 1E represents the powder X-ray diffraction spectrum of the prepared QDs. These measurements further confirmed the cubic structure. The crystal planes 111, 220 and 311 of crystalline CdS were proved by diffraction peaks at 26.75°, 44.05° and 51.95°.

Fig. 1F reveals the FT-IR spectra of free L-cysteine and L-cysteine-capped CdS QDs. By comparison of these two spectra, the most significant point to be noted is that the stretching vibration and bending mode of the S–H group at about 2552 and 942 cm^{-1} are absent in the

spectrum for QDs. The reason for absence of S–H group vibration (2550–2670 cm^{-1} wυ S–H) on the nanoparticles spectrum was the covalent bonds between the surface of CdS and thiols. It can also be seen that the IR absorption bands of the $-COO^-$ group and $-NH_2$ group were present in both spectra. This observation confirms that the two functional groups ($-NH_2$ and $-COO^-$), remain free and can be used further for conjugation with suitable biomolecules. The FE-SEM image of this QDs (Fig. 1G) exhibits that the nanoparticle has a spherical shape.

3.3. Characterization of aptamer-QDs

Fig. S1A shows the UV-Vis absorption spectrum of l-cysteine capped CdS QDs. It can be observed that QDs showed a major absorption band at around 276 nm. To confirm our assay method, fluorescence experiments were carried out. As shown in Fig. S1B, the fluorescence emission spectra of QDs and aptamer/QDs were similar. This phenomenon shows that the luminescence properties of the QDs were not influenced by the ssDNA. In addition, the maximum emission peak of QDs and aptamer-QDs were at 554 nm.

After the GO sheets were mixed with an aqueous solution containing the aptamer–QD complex, the aptamer–QD complex was bonded onto the GO sheet to form the GO/aptamer–QD ensemble, which was confirmed by the TEM observation (Fig. S1C). After interaction of GO with QDs-aptamer conjugates, many small spherical dots can be seen on the GO nano sheets. The TEM images clearly proved the successful adsorption of QDs-aptamer conjugates on the GO nano sheets. This indicated that QDs were brought close to the GO surface, further leading to the fluorescence quenching.

3.4. Optimization of detection strategy

To achieve the optimal assay performance, experimental variables, including pH and ionic strength, GO concentration, and assay time for the design of the aptasensor were first optimized.

The pH value of the solution had a great effect on the behaviour of the aptasensor. As shown in Fig. 2A(a), the effect of pH on fluorescence intensity of the QDs-aptamer/GO probe without diazinon was investigated over the pH range 5.5–9.0. When the pH of the solution increased from 5.5 to 7.0, the fluorescence quenching efficiency of GO to QDs-aptamer was enhanced, and at pH higher than 7.0, the fluorescence quenching efficiency decreased gradually. I and I_0 were the fluorescence intensity of QDs-aptamer in the presence and absence of GO, respectively. This phenomenon was seen because the carboxyl groups on the GO surface were easily deprotonated in the alkaline medium, increasing the electrostatic repulsion between GO and aptamer as a poly anion (Wu et al., 2016). Fig. 2A(b) shows the fluorescence intensity ratio of QDs-aptamer/GO assay with diazinon at different pH values and (as shown in this Figure) the maximum fluorescence intensity ratio was also achieved at pH 7.0. I and I_0 were the fluorescence intensities of the aptasensing system in the presence and absence of diazinon, respectively. The reason might be that, the higher or lower pH environments may damage the stability and activity of immobilized biomolecules and then influence the lifetime of aptasensors (Arvand & Mirroshandel., 2017; Li et al., 2013). In conclusion, pH 7.0 was chosen as the optimal pH in subsequent experiments.

The ionic strength can influence the stability of the binding of aptamer to target. It also has significant effects on the stability of the nucleic acids and GO solution. At neutral pH, the carboxyl groups on the GO surface were deprotonated. Because of the electrostatic repulsion of GO with negative charge, the polyanionic aptamer would be repelled. So, aptamer could bind to GO through hydrophobic and π–π stacking interactions. If the electrostatic repulsion was

screened by adding salts, the aptamer would be brought close to the GO surface (Li et al., 2012). We also investigated the effects of different concentrations of NaCl solution on the fluorescence intensity of the QD-aptamer/GO and QD-aptamer/GO-diazinon systems (Fig. 2B). The best quenching ratio and the optimal fluorescence recovery ratio were seen at a NaCl concentration of 150 mM. Thus this concentration of NaCl was selected as the proper ionic strength. So, 150 mM Na^+ was used in the subsequent experiments.

The potent interaction between GO and QDs-aptamer, the large specific surface area, p–p conjugated structure, good stability, water solubility, and high quenching efficiency of GO guided us to select it as the quencher. Hence, GO was very effective for construction of a fluorescence "turn off–on" mode sensor.

For achieving an optimal experimental result, the concentration of GO and the incubation time were optimized. As shown in Fig. 2C, aptamer-QDs had a narrow and symmetrical fluorescence spectrum with a maximum peak around 554 nm. It can be seen that the fluorescence intensity of aptamer-QDs decreases gradually by increasing GO concentration. The fluorescence intensity was constant when the GO concentration was higher than 270 mg l^{-1}. The maximal quenching efficiency was about 93.9%. Therefore, the GO concentration was chosen at 270 mg l^{-1}, as the optimized value for further experiments. The inset in Fig. 2C exhibits the relationship between the fluorescence intensity ratio I/I_0 and the concentration of GO (from 0 to 300 mg l^{-1}). I and I_0 were the fluorescence intensities of aptamer-QDs in the presence and absence of GO, respectively.

When 270 mg l^{-1} of GO was added to the solution, the fluorescence intensity of aptamer-QDs mixture was immediately reduced to 37.3% of the initial fluorescence intensity (Fig. 2D, curve b), which was further reduced to 6.11% after 30 min (Fig. 2D, curve c). The illustration in

Scheme 1 shows the principle of the fluorescence "turn off–on" nano sensor for diazinon detection, based on QDs-aptamer and GO.

"Please insert Scheme 1 here"

The existing fluorescent aptasensor is manufactured on the basis of the principle of FRET between the aptamer-QDs and GO. In the absence of the GO sheets, the QDs conjugated with the ssDNA aptamer in an aqueous solution exhibits strong fluorescence emission. In the presence of GO sheets, the aptamer–QD complex particles are brought into the close proximity with the surface of the GO sheet due to both π–π stacking interactions between the aromatic rings of GO and the DNA bases, and hydrogen bond formation, which occurs between hydroxyl or carboxyl groups of GO and hydroxyl or amine groups of the ssDNA aptamer (Guo & Dong, 2011; Yang et al., 2008). These factors increase the binding affinity of aptamer to GO and enable the energy transfer from the QDs to the GO sheet. As a result, the fluorescence emission of the QDs is quenched.

A control test was also done to study quenching efficiency of free l-cysteine-capped CdS QDs (without aptamer) by adding GO to the solution (Fig. 3A). It was seen that GO can interact with QDs and quench the fluorescence intensity of QDs to 35.7% after 30 min. This result indicates that, in comparison with the free QDs, the QDs–aptamer complex (100 nM) displayed a much stronger fluorescence quenching in PBS buffer after addition of 270 mg ml^{-1} GO (Fig. 3B).

In the next experiment, 270 mg l^{-1} GO was added to a mixture solution of aptamer conjugated QDs (100 nM) and diazinon (1 μM); a quenching efficiency of 22.4% was achieved

(Fig. 3C). This result shows that diazinon bonded-aptamer–QDs could not be adsorbed onto the GO sheet hindering the FRET and, therefore, this reduces the fluorescence quenching. The difference between the quenching capabilities of GO to aptamer–QDs and aptamer–QDs bound with diazinon suggested a strategy for diazinon-sensing.

In the next experiment, the kinetics of fluorescence recovery were tested in the presence of 120 nM diazinon by monitoring the fluorescence emission intensity for 1 h (Fig. S2). When the reaction time progressed, the fluorescence intensity of aptasensor initially increased rapidly and then became slow. Finally, the maximum fluorescence intensity was attained after 25 min. This was the assay time for diazinon-sensing, which was in agreement with the previous study (Alibolandi et al., 2015). The fluorescence intensity cannot completely recover to the initial fluorescence intensity of aptamer–QDs in the absence of GO in the assay (Zhou et al., 2012). Only about 91.6% of fluorescence of the aptamer–QDs was recovered.

3.5. Quantitative determination of diazinon

Different concentrations of diazinon (0.0–320 nM) were mixed into the GO/aptamer-QDs system in PBS buffer solution and the mixtures were incubated for 25 min at room temperature. Then, the fluorescence intensity was measured at 278 nm. As shown in Fig. S3A, the fluorescence intensity of the GO/aptamer-QDs ensemble gradually increased with increase in diazinon concentration. All measurements were done three times. Fig. S3B (inset) shows a good linear relationship between the fluorescence intensity I/I_0 and diazinon concentration. The linear response range of the aptasensor was determined to be 1.05–206 nM by the linear equation $I/I_0=0.0664C + 0.7655$ ($R^2=0.9972$). The detection limit of diazinon was calculated to be 0.13

nM at a signal-to-noise ratio of 3*s* (where *s* is the standard deviation of the blank solution, *n*=10). The relative standard deviation (RSD) of 11 replicate measurements at the concentration of 120 nM was 2.99%. The analytical parameters of this aptasensor are better or appropriately comparable to those previously reported, as shown in Table 1. The high sensitivity and high precision of the aptasensor may be due to the high quenching capability of GO, the remarkable difference in the affinity of aptamer toward diazinon and GO, as well as the low background signal of the fluorescent aptasensor.

3.6. Specificity analysis

Selectivity is another important parameter to evaluate the performance of the new aptasensor for detecting diazinon. To test the selectivity of this aptasensor, we recorded the fluorescence intensity variations of the GO/aptamer–QD ensemble in PBS solution after incubation with 1 μM concentrations of several common organophosphorus and organochlorine pesticides, such as heptachlor, endrin, dieldrin, edifenphos, butachlor, and chlordane for 25 min. As shown in Fig. S4, except for diazinon, all other pesticides did not show obvious effects on the fluorescence intensity of the aptasensor. It is observed that the addition of pesticides, even when their concentration is several times higher than that of diazinon, did not induce significant increase in the fluorescence of the assay system. This event is possibly attributable to the potent capacity of aptamer to bind with diazinon. Hence we can conclude that this fluorescent aptasensor based on GO has an excellent selectivity, which is sufficient for practical applications.

Moreover, the reproducibility of the proposed aptasensor was also investigated. The RSD of the responses for detection of 120 nM diazinon, using ten independently GO/aptamer–QD sensors, is 2.99 %, indicating good reproducibility. Also, no obvious change was observed for

the fluorescence intensity of the aptasensor stored at 4 °C for one week. Only a low reduction of intensity with a RSD of about 3.75% was observed, indicating the high stability of the aptasensor.

3.7. Recovery experiments

In order to evaluate the feasibility and reliability, the suggested aptasensor was applied for determining the recoveries by spiking three different concentrations of diazinon into the real surface water and agricultural samples such as cucumber and apple samples.

The samples were determined by the standard addition method and the analytical results are summarized in Table 2. As can be seen, the recoveries of the proposed aptasensor for these samples are in the range of 91.0 to 102% and the RSD was lower than 4.3%. The above results proved the feasibility of the present aptasensor for diazinon determination in environmental and agricultural samples.

4. Conclusion

In this work, a novel FRET-based aptasensor, consisting of aptamer (DF20) as biorecognition element, the L-cysteine-capped CdS QDs as donor and GO as acceptor, has been successfully designed for diazinon detection in environmental and agricultural samples with high sensitivity and specificity. The excellent quenching capability of GO reduced the fluorescence intensity of the QDs-aptamer bioconjugates by up to 93.9%. After adding diazinon, 91.6% of the fluorescence intensity was recovered because of the separation of the QDs-aptamer from the GO surface and the diazinon–aptamer-QDs complex formation. In this research, we achieved a low detection limit of 0.13 nM and an excellent linear dynamic range from 1.05 to 206 nM. This

strategy may be developed for the determination of other aptamer-specific biomolecules. In addition, aptasensors for promising prospects in the detection of different targets.

Acknowledgment

The authors are grateful to the post-graduate office of Guilan University for the support of this work.

Conflict of interest

The authors confirm that this article content has no conflict of interest.

References

Alibolandi, M., Hadizadeh, F., Vajhedin, F., Abnous, Kh., & Ramezani, M. (2015). Design and fabrication of an aptasensor for chloramphenicol based on energy transfer of CdTe quantum dots to graphene oxide sheet. *Materials Science and Engineering C*, 48, 611–619.

Arvand, M., & Mirroshandel, A. A. (2017). Highly-sensitive aptasensor based on fluorescence resonance energy transfer between l-cysteine capped ZnS quantum dots and graphene oxide sheets for the determination of edifenphos fungicide. *Biosensors & Bioelectronics*, 96, 324–331.

Barahona, F., Bardliving, C. L., Phifer, A., Bruno, J. G., & Batt, C. A. (2013). An aptasensor based on polymer-gold nanoparticle composite microspheres for the detection of malathion using surface-enhanced Raman spectroscopy. *Industrial Biotechnology*, 9, 42–50.

Bavcon, M., Trebše, P., & Zupančič-Kralj, L. (2003). Investigations of the determination and transformations of diazinon and malathion under environmental conditions using gas chromatography coupled with a flame ionization detector. *Chemosphere*, 50, 595–601.

Brodie, B. C. (1860). Production methods of graphene and resulting material properties. *Annales de Chimie et de Physique*, 59, 466–472.

Chen, Y., & Rosenzweig, Z. (2002). Luminescent CdS quantum dots as selective ion probes. *Analytical Chemistry*, 74, 5132–5138.

Dong, H., Gao, W., Yan, F., Ji, H., & Ju, H. (2010). Fluorescence resonance energy transfer between quantum dots and graphene oxide for sensing biomolecules. *Analytical Chemistry*, 82, 5511–5517.

Fahimi-Kashani, N., & Hormozi-Nezhad, M. R. (2016). Gold-nanoparticle-based colorimetric sensor array for discrimination of organophosphate pesticides. *Analytical Chemistry*, 88, 8099–8106.

Freeman, R., & Willner, I. (2012). Optical molecular sensing with semiconductor quantum dots. *Chemical Society Reviews*, 41, 4067–4085.

Gang-Il, K., Kyung-Woo, K., Min-Kyu, O., & Yun-Mo, S. (2009). The detection of platelet derived growth factor using decoupling of quencher oligonucleotide from aptamer/quantum dot bio conjugates. *Nanotechnology*, 20, 175503–175507.

Geibler, D., & Hildebrandt, N. (2016). Recent developments in Förster resonance energy transfer (FRET) diagnostics using quantum dots. *Analytical and Bioanalytical Chemistry*, 408, 4475–4483.

Guo, S., & Dong, S. (2011). Graphene and its derivative-based sensing materials for analytical devices. *Journal of Materials Chemistry A*, 21, 18503–18516.

Guo, J., Luo, Y., Li, H., Liu, X., Bie, J., Zhang, M., Cao, X., Shen, F., Sun, C., & Liu, J. (2013). Sensitive fluorescent detection of carbamate pesticides represented by methomyl based on the inner filter effect of Au nanoparticles on the fluorescence of CdTe quantum dots. *Analytical Methods*, 5, 6830–6838.

Hossain, S. M. Z., Luck ham, R. E., McFadden, M. J., & Brennan, J. D. (2009). Reagentless bidirectional lateral flow bioactive paper sensors for detection of pesticides in beverage and food samples. *Analytical Chemistry*, 81, 9055–9064.

Huang, S., Zhu, F., Qiu, H., Xiao, Q., Zhou, Q., Su, W., & Hu, B. (2014). A sensitive quantum dots based "OFF–ON" fluorescent sensor for ruthenium anticancer drugs and ctDNA. *Colloids and Surfaces B: Biointerfaces*, 117C, 240–247.

Jiao, Y., Jia, H., Guo, Y., Zhang, H., Wang, Z., Sun, X., & Zhao, J. (2016). An ultrasensitive aptasensor for chlorpyrifos based on ordered mesoporous carbon/ferrocene hybrid multiwalled carbon nanotubes. *RSC Advances*, 6, 58541–58548.

Jokar, M., Safaralizadeh, M. H., Hadizadeh, F., Rahmani, F., & Kalani, M. R. (2017). Apta-nano-sensor preparation and in vitro assay for rapid diazinon detection using a computational molecular approach. *Journal of Biomolecular Structure & Dynamics*, 35, 343–353.

Karnati, C., Du, H. W., Ji, H. F., Xu, X. H., Lvov, Y., Mulchandani, A., Mulchandani, P., & Chen, W. (2007). Organophosphorus hydrolase multilayer modified microcantilevers for organophosphorus detection. *Biosensors & Bioelectronics*, 22, 2636–2642.

Kwon, Y. S., Nguyen, V. T., Park, J. G., & Gu, M. B. (2015). Detection of iprobenfos and edifenphos using a new multi-aptasensor. *Analytica Chimica Acta*, 868, 60–66,

Li, F., Feng, Y., Zhao, C., Li, P., & Tang, B. (2012). A sensitive graphene oxide–DNA based sensing platform for fluorescence "turn-on" detection of bleomycin. *Chemical Communications*, 48, 127–129.

Li, W., Zhang, Q., Zhou, H., Chen, J., Li, Y., Zhang, C., & Yu, C. (2015). Chemiluminescence detection of a protein through the aptamer-controlled catalysis of a porphyrin probe. *Analytical Chemistry*, 87, 8336–8341.

Li, M., Zhou, X., Guo, S., & Wu, N. (2013). Detection of lead (II) with a "turn-on" fluorescent biosensor based on energy transfer from CdSe/ZnS quantum dots to graphene oxide. *Biosensors & Bioelectronics*, 43, 69–74.

Liu, Z., Tian, C., Lub, L., & Su, X. (2016). A novel aptamer-mediated $CuInS_2$ quantum dots@graphene oxide nanocomposites-based fluorescence "turn off–on" nanosensor for highly sensitive and selective detection of kanamycin. *RSC Advances*, 6, 10205–10214.

Ma, J., Xiao, R., Li, J., Zhao, X., Shi, B., & Li, S. (2009). Determination of organophosphorus pesticides in underground water by SPE-GC-MS. *Journal of Chromatographic Sciences*, 47, 110–114.

Motaharian, A., Motaharian, F., Abnous, Kh., Milani Hosseini, M. R., & Hassanzadeh-Khayyat, M. (2016). Molecularly imprinted polymer nanoparticles-based electrochemical sensor for determination of diazinon pesticide in well water and apple fruit samples. *Analytical and Bioanalytical Chemistry*, 408, 6769–6779.

Saraji, M., Rezaei, B., Boroujeni, M. K., & Bidgoli, A. A. H. (2013). Polypyrrole/sol-gel composite as a solid-phase microextraction fiber coating for the determination of organophosphorus pesticides in water and vegetable samples. *Journal of Chromatography A*, 1279, 20–26.

Sheng, W., Chen, T., Kamath, R., Xiong, X., Tan, W., & Fan, Z. H. (2012). Aptamer-enabled efficient isolation of cancer cells from whole blood using a microfluidic device. *Analytical Chemistry*, 84, 4199–4206.

Shi, J., Tian, F., Lyu, J., & Yang, M. (2015). Nanoparticle based fluorescence resonance energy transfer (FRET) for biosensing applications. *Journal of Materials Chemistry B*, 3, 6989–7005.

Sotiropoulou, S., Fournier, D., & Chaniotakis, N. A. (2005). Genetically engineered acetylcholinesterase-based biosensor for attomolar detection of dichlorvos. *Biosensors & Bioelectronics*, 20, 2347–2352.

Sullivan, J. J., & Goh, K. S. (2000). Evaluation and validation of a commercial ELISA for diazinon in surface waters. *Journal of Agricultural and Food Chemistry*, 48, 4071–4078.

Tang, Y., Zhang, J., Liu, J. H., Gapparov, L., Wang, S., Dong, Y., Sua, H., & Tana, T. (2017). The development of a graphene oxide-based aptasensor used for the detection of tetracycline in honey. *Analytical Methods*, 9, 1133–1140.

Treossi, E., Melucci, M., Liscio, A., Gazzano, M., Samorı, P., & Palermo, V. (2009). High-contrast visualization of graphene oxide on dye-sensitized glass, quartz, and silicon by fluorescence quenching. *Journal of the American Chemical Society*, 131, 15576–15577.

Vamvakaki, V., & Chaniotakis, N. A. (2007). Pesticide detection with a liposome-based nano-biosensor. *Biosensors & Bioelectronics*, 22, 2848–2853.

Wu, J., Hou, Y., Wang, P., Wang, Z., Li, Y., Wang, S., & Yang, M. (2016). Detection of lysozyme with aptasensor based on fluorescence resonance energy transfer from carbon dots to graphene oxide. *Luminescence*, 31, 1207–1212.

Yan, X., Li, H., Wang, X., & Su, X. (2015). A novel fluorescence probing strategy for the determination of parathion-methyl. *Talanta*, 131, 88–94.

Yang, W., Wu, Y., Tao, H., Zhao, J., Chen, H., & Qiu, Sh. (2017). Ultrasensitive and selective colorimetric detection of acetamiprid pesticide based on the enhanced peroxidase-like activity of gold nanoparticles. *Analytical Methods*, 9, 1–9.

Yang, X., Zhang, X., Liu, Z., Ma, Y., Huang, Y., & Chen, Y. (2008). High efficiency loading and controlled release of doxorubicin hydrochloride on graphene oxide. *Journal of Physical Chemistry C*, 112, 17554–17558.

Zhang, Y., & Wang, T. H. (2012). Quantum Dot enabled molecular sensing and diagnostics. *Theranostics*, 2, 631–654.

Zhao, Y., Ma, Y., Li, H., & Wang, L. (2012). Composite QDs@MIP nanospheres for specific recognition and direct fluorescent quantification of pesticides in aqueous media. *Analytical Chemistry*, 84, 386–395.

Zhou, C., Wang, T., Liu, J., Guo, C., Peng, Y., Bai, J., Liu, M., Dong, J., Gao, N., Ning, B., & Gao, Z. (2012). Molecularly imprinted photonic polymer as an optical sensor to detect chloramphenicol. *Analyst*, 137, 4469–4474.

Table 1

Performance comparison of the novel method with other previously reported sensors for pesticide detection

Type of sensor	Analyte	Dynamic range (nM)	LOD (nM)	RSD (%)	Ref.
QDs-MIP composite/fluorescence sensor	Diazinon	164–1970	164	1.1	(Zhao et al., 2012)
Aptamer + AgNPs/colorimetric method	Diazinon	0.141–0.65	17.9	2.6	(Motaharian et al., 2016)
MIP NPs/electrochemical sensor	Diazinon	2.5–100	0.79	–	(Jokar et al., 2017)
Enhanced peroxidase + AuNps /colorimetric method	Acetamiprid	44–718	4.5	1.8–4.6	(Yang et al., 2017)
AuNps /colorimetric sensor array	Azinphos-methyl	252–1260	236	–	(Fahimi-Kashani & Hormozi-Nezhad, 2016)
AuNps + CdTe quantum dots/fluorescence sensor	Carbamate	0.283 –8300	183	4.3	(Guo et al., 2013)
Aptasensor + polymer- AuNps composite microspheres	Malathion	9.98–100.79 μM	0.9 μM	14	(Barahona et al., 2013)
AuNPs + aptamer/colorimetric method	EDI	5–25	5	8.1	(Kwon et al., 2015)
CdTe QDs + organophosphorus hydrolase/fluorescence probing	Parathion-methyl	0.094–11.3 μM	68.38	5.1	(Yan et al., 2015)
Aptasensor+ mesoporous carbon/ferrocene hybrid MWCNTs	Chlorpyrifos	2.8 nM–0.28 mM	0.94	4.3	(Jiao et al., 2016)
L-cysteine-capped-CdS QDs + aptamer/fluorescence spectroscopy	Diazinon	1.05–205.83	0.13	2.99	This work

Table 2

Analysis of real samples with the proposed fluorescent aptasensor

Sample	Added (nM)	Detected (mean, *n*=3)	Recovery (%)
River water	10	9.3 ± 2.6	93.0
Shafa-rood (Guilan, Iran)			
	50	50.8 ± 3.1	102
	100	99.3 ± 2.2	99.3
Apple fruit	10	9.1 ± 3.7	91.0
	50	48.5 ± 3.9	97.0
	100	96.1 ± 4.3	96.1
Cucumber	10	9.1 ± 2.8	91.0
	50	49.2 ± 3.0	98.4
	100	97.8 ± 2.9	97.8

n is the repetitive measurement number.

Scheme caption

Scheme 1. The principle of the fluorescence "turn off–on" aptasensor for diazinon detection based on QDs-aptamer and GO.

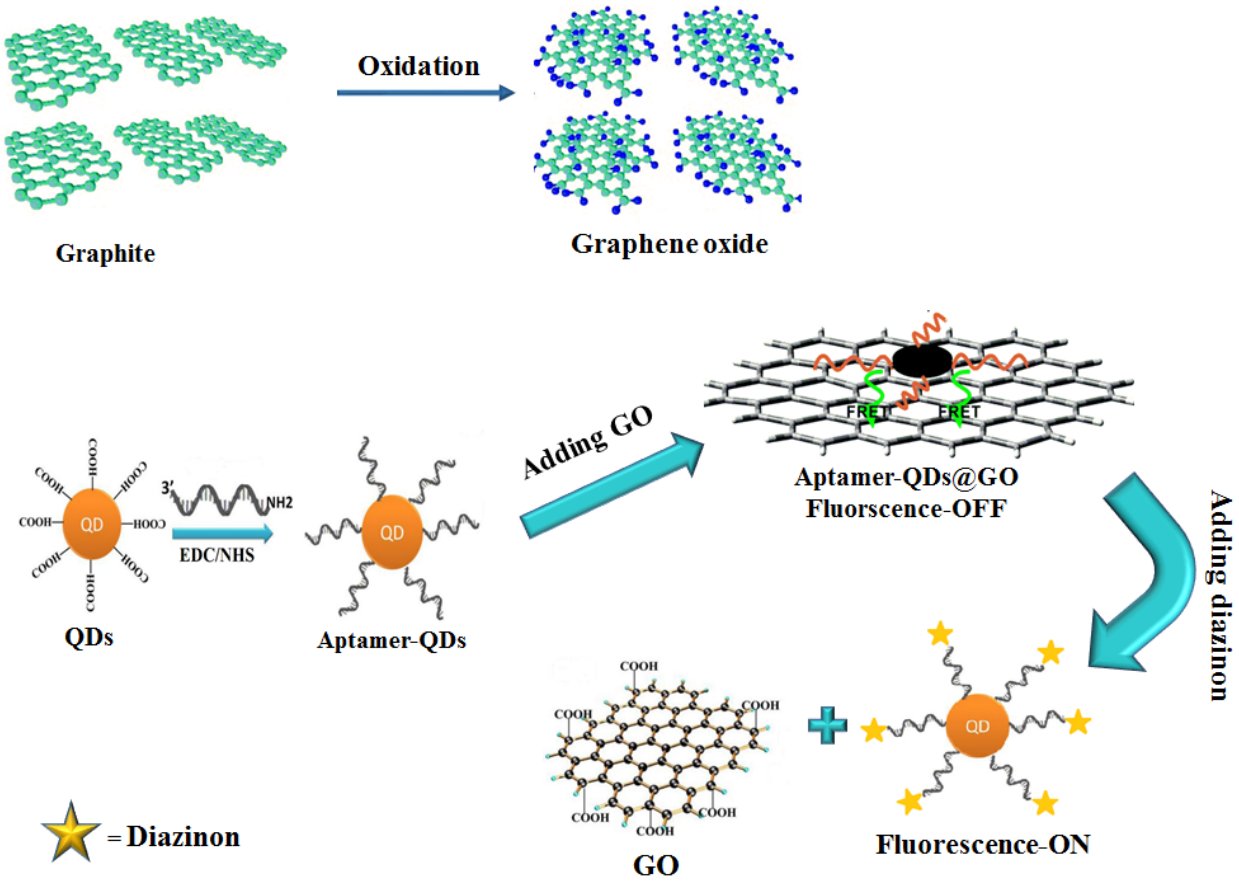

Scheme 1

Figure captions

Fig. 1. (A) FT-IR spectra of graphite (a) and graphene oxide (b); (B) TEM image of GO; (C) SEM image of GO. (D) TEM image of L-cysteine-capped CdS QDs; (E) X-ray diffractogram of QDs; (F) FT-IR spectra of free L-cysteine (a) and L-cysteine-capped CdS QDs (b); (G) FE-SEM image of QDs.

Fig. 2. (A) Effect of pH value on the fluorescence quenching efficiency of GO to QDs-aptamer without diazinon (a) and the fluorescence intensity ratio of QDs-aptamer/GO probe with diazinon (b); (B) Effect of NaCl concentration on the fluorescence quenching efficiency of GO to QDs-aptamer (a) and the fluorescence intensities ratio of QDs-aptamer/GO probe with diazinon (b) (I and I_0 are the fluorescence intensity of aptamer-QDs in the presence and absence of GO (RSD=2.99%), respectively). (C) The fluorescence spectra of aptamer-QDs in the presence of different concentrations of GO (0.0, 55, 112, 168, 208, 228, 250, 270, 300 mg l^{-1}). (D) Fluorescence emission spectra of aptamer-QDs (100 nM) in PBS (a), aptamer-QDs in PBS incubated with 270 mg l^{-1} GO for 5 min (b), aptamer-QDs incubated with 270 mg l^{-1} GO for 30 min (c).

Fig. 3. (A) Fluorescence emission spectra of QDs (100 nM) in PBS solution; (B) Aptamer-QDs (100 nM) in PBS solution; (C) Aptamer-QDs (100 nM) in PBS solution with 1 μM diazinon (a) before and (b) after adding 270 mg l^{-1} GO.

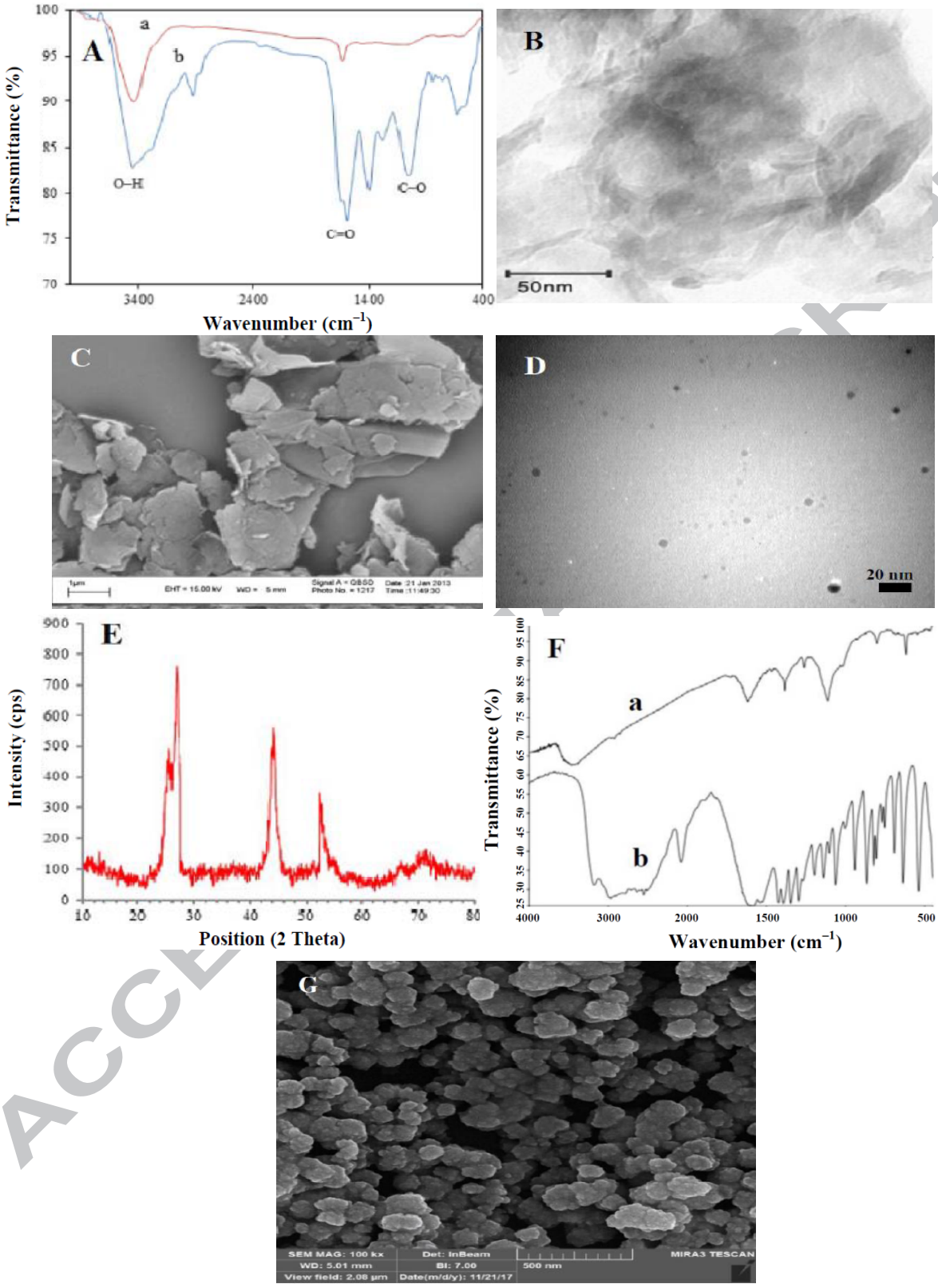
A
a
b
O–H
C=O
C–O
Transmittance (%)
Wavenumber (cm^{-1})
B
50nm
C
D
20 nm
E
Intensity (cps)
Position (2 Theta)
F
a
b
Transmittance (%)
Wavenumber (cm^{-1})
G
SEM MAG: 100 kx
WD: 5.01 mm
View field: 2.08 µm
Det: InBeam
BI: 7.00
Date(m/d/y): 11/21/17
500 nm
MIRA3 TESCAN

Fig. 1

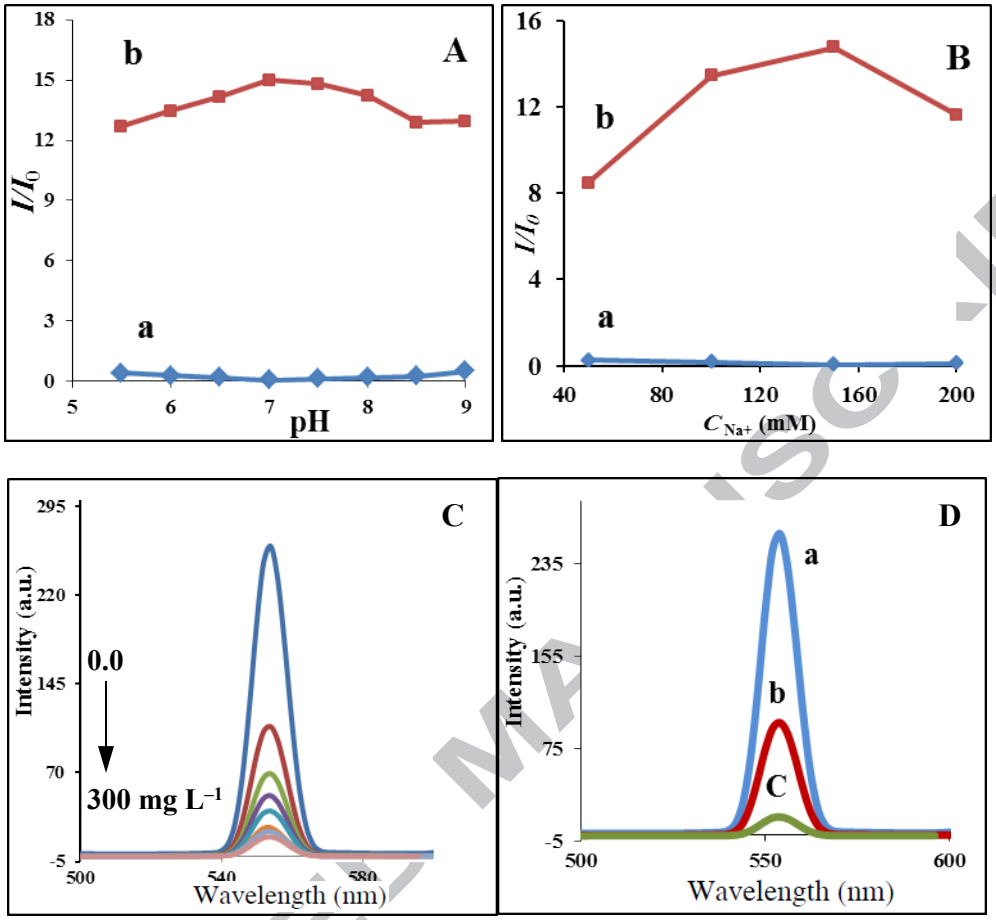

Fig. 2

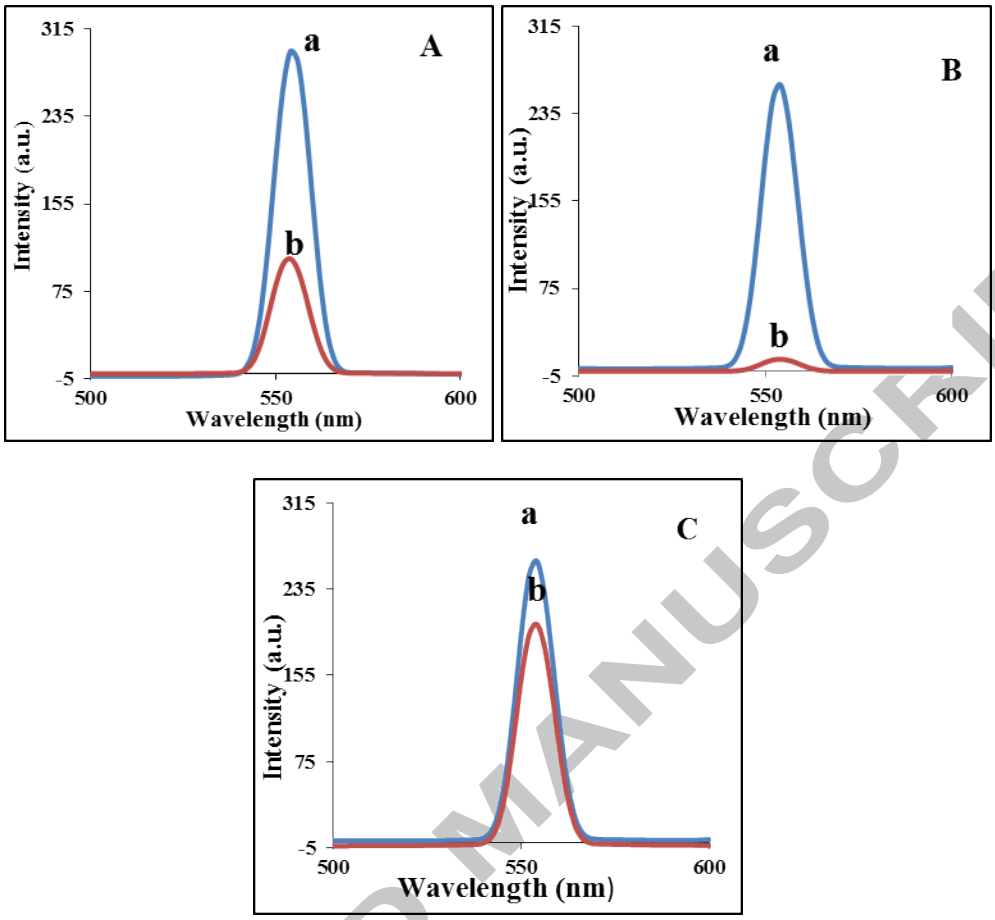

Fig. 3

Highlights

- A simple, sensitive and selective fluorescence aptasensor based on FRET for diazinon is achieved.
- ss-DNA (aptamer) is applied as the biorecognition element and improves the selectivity remarkably.
- The fluorescence FRET aptasensor achieves a limit of detection to 0.13 nM diazinon
- Diazinon detection in environmental and agricultural samples exhibits good reliability and stability